NASA/CR – 1998   206767

The Onset of the 1997-98 El Niño and its Impact on the Phytoplankton Community of the Central Equatorial Pacific

Francisco P. Chavez, Peter G. Strutton and Michael J. McPhaden

Using physical and bio-optical data from moorings in the central equatorial Pacific, the perturbations to phytopankton biomass and productivity associated with the onset of the 1997-98 El Niño event were investigated. The data presented depict the physical progression of El Niño onset, from reversal of the trade winds in the western equatorial Pacific, through eastward propagation of equatorially trapped Kelvin waves and advection of waters from the nutrient-poor western equatorial warm pool. The physical perturbations led to fluctuations in phytoplankton biomass, quantum yield of fluorescence and a 50% reduction in primary productivity.

Equatorial upwelling, driven by the trade winds that blow from east to west, results in sea surface temperatures in the central and eastern equatorial Pacific that are abnormally cool for a tropical ocean. This upwelling of cool, nutrient-rich waters has consequences not only for global climate, but also for biogeochemical cycles (1-3). During cool periods the equatorial Pacific is the largest natural source of carbon dioxide (2) to the atmosphere, and accounts for a fifth of the global supply of nitrate to surface waters (4). The degassing of carbon dioxide from ocean to atmosphere can be linked to low rates of new production (5) so that a positive gradient of carbon dioxide between ocean and atmosphere is almost permanently maintained (6). These low rates of new production are a result of iron limitation (7), with silicate acting as a

---

F.P. Chavez, P.G. Strutton, Monterey Bay Aquarium Research Institute, PO Box 628, Moss Landing, CA 95039, USA
M.J. McPhaden, NOAA/PMEL, 7600 Sand Point Way NE, Seattle, WA 98115, USA

1

secondary regulator (8).

Approximately every three to eight years, equatorial Pacific sea surface temperatures become anomalously warm in association with El Niño, a phenomenon with global climatic implications (9). While the physical and climatic consequences of El Niño are relatively well understood the biological consequences in the equatorial Pacific are still poorly determined. In this report we present a time series of bio-optical measurements collected during the onset of the 1997-98 El Niño, a particularly strong event. We present evidence for strong physical-biological coupling and suggest that primary production was reduced to 50% of that observed during the climatological mean.

Our current level of understanding regarding the physical processes associated with El Niño has been in part facilitated by the Tropical Atmosphere Ocean (TAO) array. The array consists of approximately 70 moored buoys across the equatorial Pacific Ocean (10, 11). These buoys record surface air temperature, wind velocity and humidity, and ocean temperature to a depth of 500 m, and transmit data daily, thus facilitating near real-time monitoring and prediction of basin scale physical changes associated with El Niño. In late 1996 bio-optical instrumentation was installed on moorings located at 0°, 155°W and 2°S, 170°W to monitor the biological changes associated with El Niño as well as validate ocean color satellites. Here we present the bio-optical data from 0°, 155°W (subsequently referred to as the mooring site) to illustrate the effect of onset of the 1997-98 El Niño on the phytoplankton community of the equatorial Pacific.

Time/longitude sections of anomalies in surface zonal winds, sea surface temperature (SST) and 20°C isotherm depth (a proxy for the thermocline) are used to describe the onset and development of the 1997-98 El Niño (Figure 1). Anomalous westerly winds were first observed in the western Pacific in December 1996/January 1997. These westerly wind bursts, associated with the 30 to 60 day Madden-Julian Oscillation (12), generated Kelvin waves that propagated across the Pacific at over 200 km day^{-1}, raising sea level and deepening the thermocline (Figure 1B). The anomalies in SST

2

did not begin in earnest until after the second set of wind anomalies in March and April 1997 (Figure 1C). The lag between subsurface and surface anomalies suggests that the surface effects were associated with either vertical or lateral advection. The relative importance of these mechanisms is dictated in part by longitude; in the western Pacific, advection of water from the warm pool is dominant (13, 14), while in the east, downwelling accounts for much of the observed anomaly (15). The increase in the SST anomaly of approximately 2°C from March to May 1997 at the mooring site (Fig. 1C) was likely a combination of these two processes.

The time series of bio-optical properties began in early December 1996, prior to the first set of wind anomalies (Figure 1A). The first signature of subsurface anomalies was observed at the mooring site in January 1997 (Figure 1B). A recovery of the thermocline was observed in February 1997 prior to arrival of the second Kelvin wave in March 1997. During the observation period the local winds at the mooring site remained normal and upwelling favorable (Figures 1A and 2A). Clearly, the subsurface anomalies at 0°, 155°W were not associated with variations in the local winds but were forced remotely from the western Pacific. Similarly, the low frequency variations in chlorophyll and primary production are coherent with variations in subsurface anomalies, and not with variations in the local winds (Figures 2B and 3). We hypothesize that fluctuations in phytoplankton biomass and production (Figures 2 and 3) are associated with variations in the flux of iron into the euphotic zone (6, 16, 17).

During normal conditions, waters from the Equatorial Undercurrent (EUC) are upwelled along the equatorial Pacific (18) and are the most important source of iron for surface waters (19). The upwelled iron leads to a very narrow region of enhanced biological productivity tightly focused around the equator (6, 16). However, the iron source is small relative to the macronutrients (nitrate, phosphate) upwelled and a large pool of these remains at the surface once the iron is consumed. If the Kelvin waves deepen the EUC (Figure 4) but not the depth from which upwelled water is recruited (~60-

100 m) then the supply of iron to the euphotic zone should be dramatically reduced. The result is a decrease in biological productivity and unused macronutrients at the equator. The calculated NO_3 concentration of ~3.0 μM (20) at the mooring site in May 1997 (Figure 3C) agrees extremely well with the values of 2.9 to 3.1 μM measured on samples collected during the mooring recovery cruise. The estimated concentration of nitrate showed little variation prior to April, was well above levels found in oligotrophic waters (<0.1 μM) and was less coherent with the chlorophyll and primary productivity time series than the time series of the depth of the 20°C isotherm.

Two approaches were used to investigate phytoplankton growth during the time period of bio-optical measurements. The first involved calculation of the intrinsic growth rate (k) of the population from net growth and grazing. The net phytoplankton growth coefficient was calculated as $\mu = \ln(Chl_{t+1}/Chl_t)$ [day^{-1}]. Grazing rate was estimated from a relationship between chlorophyll and grazing rate derived from the pooled grazing experiment data for the equatorial Pacific (21, 22). We feel it is appropriate to use this approach for the equatorial Pacific because it is a microbial loop dominated system (6). The intrinsic growth rate is then the sum of net growth and grazing rate. Growth rate (k) co-varied with the depth of the 20°C isotherm and fluctuated between 0.5 and 0.8 day^{-1} (Figure 3B); consistent with empirical data from the equatorial Pacific at 140°W (6, 23). A second estimate of growth or physiological status is the quantum yield of fluorescence (Φ_f), calculated using the mean chlorophyll concentration in the upper 20 m and the upwelling radiance at 683 nm from 20 m (24). Φ_f is related in an approximately inverse fashion to the quantum yield of photosynthesis and is used here as an inverse measure of photosynthetic efficiency. The quantum yield also co-varies with the depth of the 20°C isotherm (Figure 3B). Thus, two independent estimates show the effects of Kelvin wave propagation, presumably through iron supply, on phytoplankton growth.

The SST time series indicates that the 28°C isotherm, which can be used as a marker for the eastern edge of the warm pool (14), moved eastwards past the mooring site in

4

late April 1997, after the passing of the second Kelvin wave. These warmer waters are traditionally associated with very low nitrate concentrations (25). It is proposed that the advection of macronutrient-poor waters into the region of the mooring, in concert with reduced vertical flux of iron, caused the dramatic decrease in the photosynthetic rate (manifested as an increase in the quantum yield of fluorescence) and the steep decline in phytoplankton productivity in late April. Had observations extended into May and June we would predict even stronger chlorophyll and productivity anomalies at 0°, 155°W as macronutrients approached zero.

While these are not the first time series observations from the equatorial Pacific, the timing and location of the measurements has helped to identify the response of the phytoplankton community to distinct physical processes; Kelvin wave propagation, upwelling and zonal advection. Time series of three weeks or less showed correlation between pigment concentrations and meridional (north-south) current variation associated with the passing of tropical instability waves at 0°, 140°W (17). On longer temporal scales, a 400-day record of bio-optically derived primary productivity, correlated extremely well with ship based measurements using standard ^{14}C techniques (26). Large scale variability associated with the passage of tropical instability waves and Kelvin waves was observed, but due to their overlapping time scales, the relative contribution of these physical phenomena to biological variability could not be unambiguously determined.

Mean primary production in the equatorial Pacific is approximately 900 mg C m^{-2} day^{-1} (6), which is well within the range of our derived values in Fig. 3A. The drop in production in late April 1997 suggests that the onset of El Niño depressed primary production by as much as 50% from the mean. At 140°W, a similar 50% decrease in integrated primary productivity was observed (16) associated with the 1991-1992 El Niño. While fluctuations of this magnitude have significant consequences for the interannual variation in biogeochemical processes, recent work has suggested that

global climate and equatorial Pacific biological variation may be linked on longer temporal scales.

On glacial-interglacial time scales, barite cores from the equatorial Pacific sea floor along 140°W indicate a strong link between climatic cycles and equatorial Pacific primary productivity over the last 450,000 years (27). Using an empirical relationship between barite ($BaSO_4$) accumulation and the productivity of the overlying water column, primary productivity in interglacial periods was found to be approximately half that of glacial periods. The range of productivity values between glacial and interglacial conditions was strikingly similar to that shown in Figure 3. While the processes driving glacial-interglacial variations in primary productivity remain unresolved, one scenario might be that interglacial periods exhibit higher frequencies of El Niño events compared to glacial periods.

The description of the extent and nature of the bio-physical coupling during the evolution of El Niño was only possible because of continuous time series. Comparison of the 5-day and 21-day moving averages of chlorophyll and primary production (Figure 3A) shows that single occupations can be severely aliased by higher frequency variability, most likely related to variations in local processes. These data illustrate the potential for bio-optical time series of this type, combined with concurrent atmospheric and oceanographic data, to enhance our understanding of the biogeochemical processes associated with basin scale oceanographic fluctuations. Satellite observations of ocean color would have provided a valuable complement to the moored time series. With the recent launch of SeaWiFS documenting the progression and recovery from El Niño will now be possible from moorings and satellites. Given the coupling between physical and biological processes presented here, bio-optical data exhibit great potential for quantifying the long-term interactions between global climate and biogeochemical cycles.

References

1. F.P. Chavez and R.T. Barber, *Deep-Sea Res.* **34**, 1229 (1987).

2. R.A. Feely *et al.*, *J. Geophys. Res.* **92**, 6545 (1987).

3. J.W.Murray, R.T. Barber, M.R. Roman, M.P. Bacon, R.A. Feely, *Science* **266**, 58 (1994).

4. F.P. Chavez and J.R. Toggweiler, in *Upwelling in the Ocean: Modern Processes and Ancient Records*, C.P. Summerhayes, K.-C. Emeis, M.V. Angel, R.L. Smith and B. Zeitzschel, Eds. (Wiley, New York, 1995), chap. 15.

5. R.C. Dugdale and J.J. Goering, *Limnol. Oceanogr.* **12**, 196 (1967).

6. F. P. Chavez, K.R. Buck, S.K. Service, J. Newton, R.T. Barber, *Deep-Sea Res. II*, **43**, 835 (1996).

7. K. H. Coale, *et al.*, *Nature* **383**, 495 (1996).

8. R.C. Dugdale and F.P. Wilkerson, *Nature,* in press.

9. E.M. Rasmusson and J.M. Wallace, *Science* **222**, 1195 (1983).

10. M.J. McPhaden, *Oceanography* **6**, 36 (1993).

11. M.J. McPhaden, *Bull. Am. Meteorol. Soc.* **76**, 739 (1995).

12. R.A. Madden and P.R. Julian, *J. Atmos. Sci.* **28**, 702 (1971).

13. M.J. McPhaden and J. Picaut, *Science* **250**, 1385 (1990).

14. J. Picaut, M. Ioualalen, C. Menkes, T. Delcroix, M.J. McPhaden, *Science* **274**, 1486 (1996).

15. W.S. Kessler and M.J. McPhaden, *Deep-Sea Res. II* **42**, 295 (1995).

16. R.T. Barber *et al.*, *Deep-Sea Res. II* **43**, 933 (1996).

17. R.R. Bidigare and M.E. Ondrusek, *Deep-Sea Res. II* **43**, 809 (1996).

18. J.R. Toggweiler and S. Carson, in *Upwelling in the Ocean: Modern Processes and Ancient Records*, C.P. Summerhayes, K.-C. Emeis, M.V. Angel, R.L. Smith and B. Zeitzschel, Eds. (Wiley, New York, 1995), chap. 17.

19. K. H. Coale, S.E. Fitzwater, R.M. Gordon, K.S. Johnson, R.T.Barber, *Nature* **379**, 621 (1996).

20. The nitrate (NO_3) concentration at 0°, 155°W for the period corresponding to our bio-optical measurements was calculated from SST using a quadratic relationship derived for the region 1°N to 1°S, 180°W to 95°W; F.P. Chavez, S.K. Service, S.E. Buttrey, *J. Geophys. Res.* **101**, 20553 (1996).

21. M.R. Landry, J. Constantinou, J. Kirshtein, *Deep-Sea Res. II* **42**, 657 (1995).

22. P.G. Verity, D.K. Stoecker, M.E. Sieracki, J.R. Nelson, *Deep-Sea Res. II* **43**, 1227 (1996).

23. D. Vaulot, D. Marie, R.J. Olson, S.W. Chisholm. *Science*, **268**, 1480 (1995).

24. W.S. Chamberlin, C.R. Booth, D.A. Kiefer, J.H. Morrow, R.C. Murphy, *Deep-Sea Res.* **37**, 951 (1990).

25. D.J. Mackey, J. Parslow, H.W. Higgins, F.B. Griffiths, J.E. O'Sullivan, *Deep-Sea Res. II* **42**, 499 (1995).

26. D.G. Foley, *et al.,Deep-Sea Res II.* In press

27. A. Paytan, M. Kastner, F.P. Chavez, *Science* **274**, 1355 (1996).

28. J.T.O. Kirk, *Light and Photosynthesis in Aquatic Ecosystems* (Cambridge University Press, 1994).

29. A. Morel, *J. Geophys. Res.* **93**, 10749 (1988).

30. W.S. Kessler, M.C. Spillane, D.E. Harrison, M.J. McPhaden, in *Proceedings of the International Scientific Conference on the Tropical Ocean Global Atmosphere (TOGA) Programme*, (Melbourne, Australia, 2-7 April 1995), *pp* 210-214.

Figure legends

Figure 1: Time/longitude sections of anomalies in **(A)** surface zonal winds (m s^{-1}), **(B)** 20°C isotherm depth (m) and **(C)** SST (°C) for 24 months ending in October of 1997. Analysis is based on 5-day averages between 2°N and 2°S of moored time series data from the TAO array. Anomalies are relative to monthly climatologies cubic spline fitted to 5-day intervals. Squares on the abscissas indicate longitudes where data were available. Major anomalies in the western Pacific wind field occur on a 30-60 day cycle (*12*) beginning in December 1996. Each "burst" of westerlies generates a Kelvin wave that can be traced in the depth of the 20°C isotherm as it propragates across the Pacific at over 200 km day^{-1}. The SST anomalies lag the subsurface perturbations and are notable after April 1997. The time series of bio-optics was collected at 0°, 155°W from December 1996 to May 1997 (denoted by a cleared strip in the time/longitude sections).

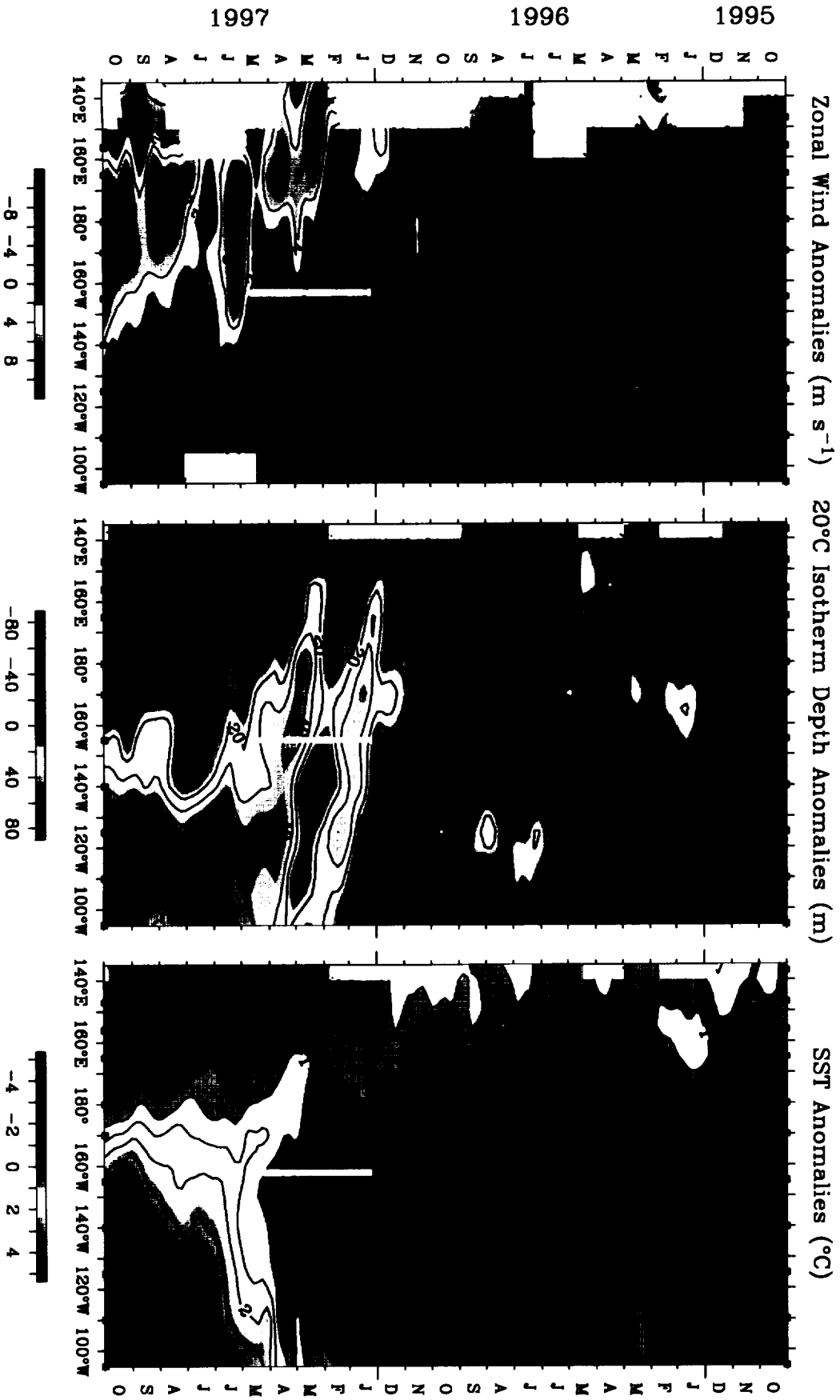**Figure 2. (A)** Time series of the zonal (east-west) wind vector at 0°, 155°W for the period May 12th, 1996 to May 12th, 1997. Negative values represent winds originating from the east and are upwelling favorable. 21 day moving averages of the original data are plotted for ease of interpretation. In all figures, the abscissa labels represent the first day of the relevant month. **(B)** 21-day moving average of the depth of the 20°C isotherm (———) and chlorophyll (—   —). The r^2 between wind and chlorophyll is 0.04 and for isotherm and chlorophyll 0.69 (n=133). Downwelling solar irradiance data recorded 3 m above the surface and at 20 m depth were used to calculate the diffuse attenuation coefficient (*28*) at 490 nm (K_{490}), which was then converted to a mean chlorophyll concentration for the upper 20 m of the water column (*29*). The sensor at 20 m depth was protected from bio-fouling by a copper "shutter" that opened on command prior to each measurement and remained closed in between measurements.
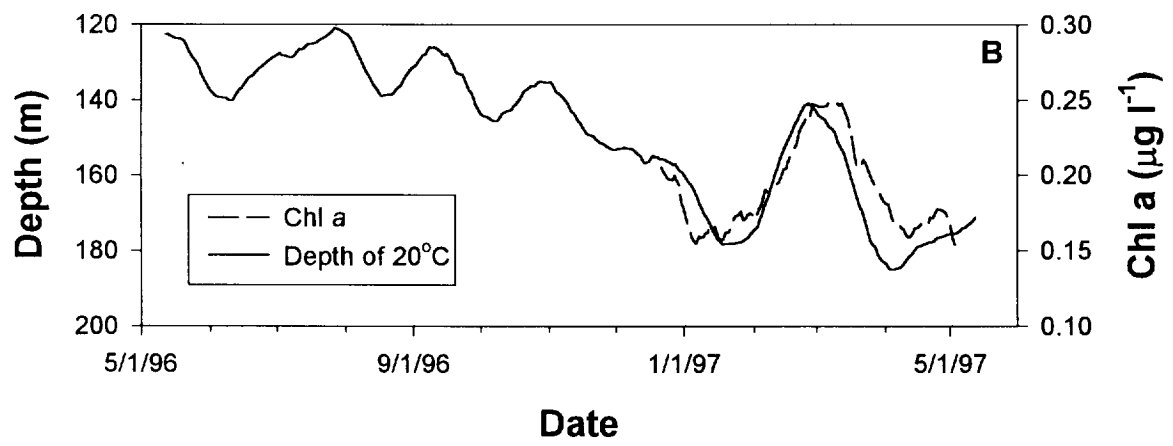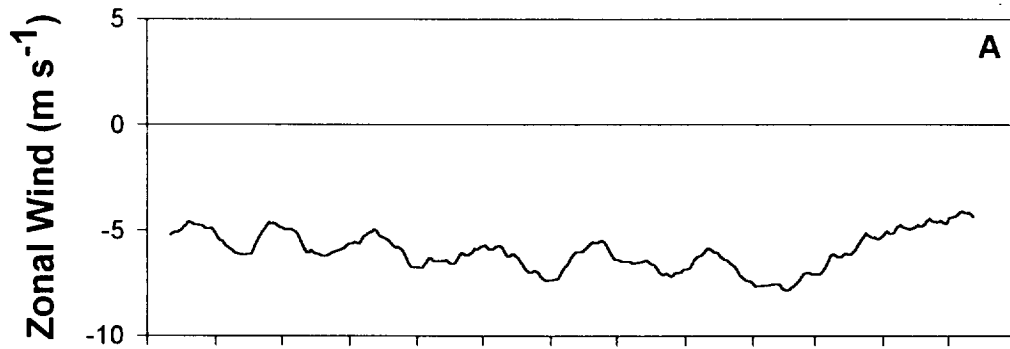
Figure 3: (A) Time series of mean chlorophyll a concentration for the upper 20 m of the water column, calculated from K_{490} (*29*), for the period Dec 11th, 1996 to May 12th, 1997. Five day (———) and 21 day (—   —) moving averages of daily data are plotted.
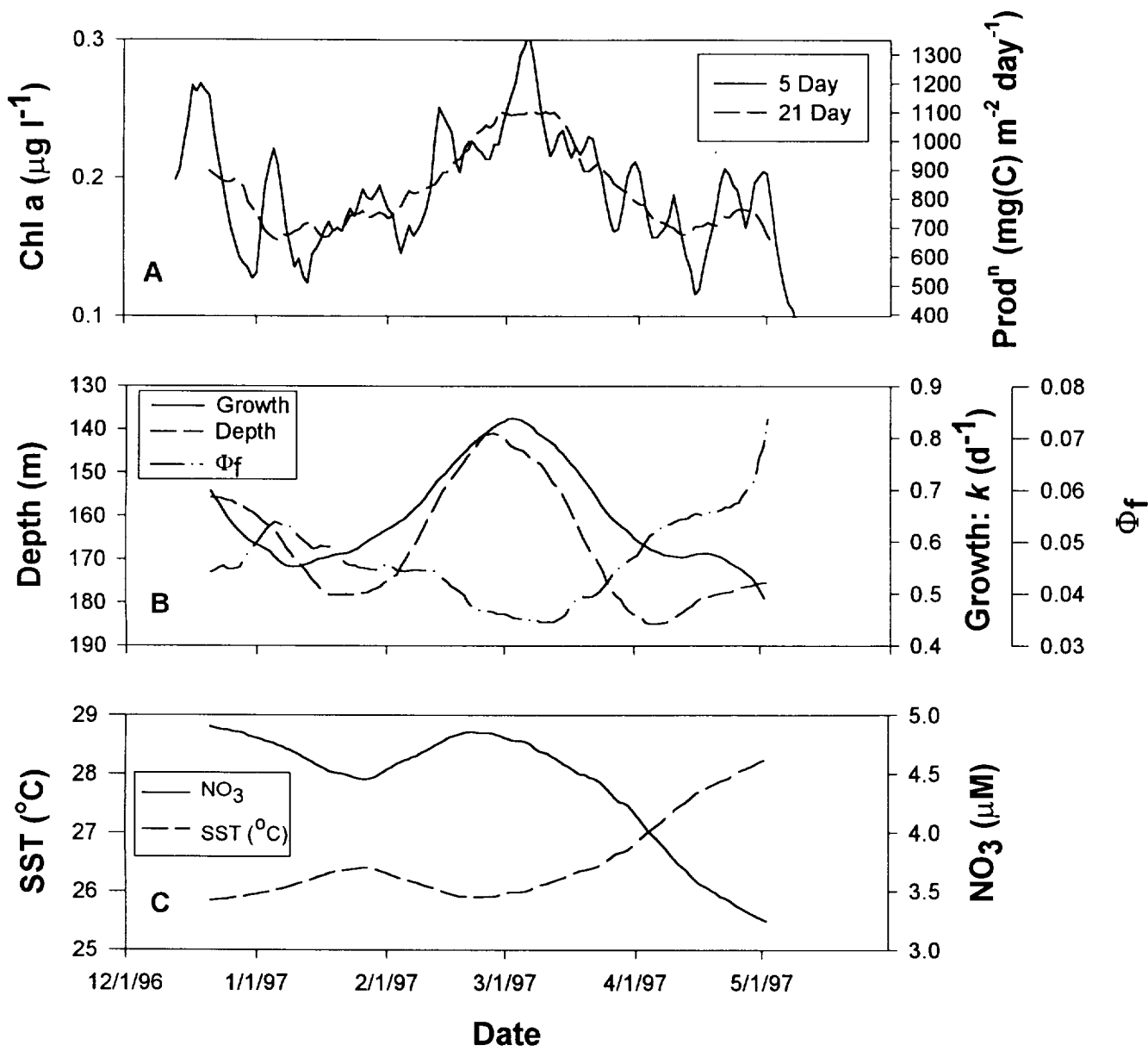
10

Primary productivity was calculated from a regression between surface chlorophyll and primary productivity (r^2=0.64, n=56) measured on JGOFS cruises (http://www1.whoi.edu/jgofs.html) **(B)** 21 day moving average of the depth of the 20°C isotherm (— —), phytoplankton growth (——) and quantum yield of fluorescence, Φ_f (— . —). The r^2 between growth and Φ_f = 0.80 (n=133). **(C)** 21 day moving average of the surface nitrate concentration (——) calculated from sea surface temperature (— —) [20].

Figure 4. Time series of zonal velocity from an Acoustic Doppler Current Profiler moored at 0°, 170°W for the period August 1996 to May 1997. Eastward velocity is positive. The core of the Equatorial Undercurrent steadily deepens from 100 m to 200 m by March 1997. We surmise similar changes at 0°, 155°W based on coherence scales of at least 15° longitude for intraseasonal and interannual zonal velocity variations along the equator [30].

Five Day Mean Zonal Wind, 20°C Isotherm Depth, and SST 2°S to 2°N Average

Zonal Wind Anomalies (m s⁻¹)

20°C Isotherm Depth Anomalies (m)

SST Anomalies (°C)

Nov 4 1997

Depth (m)

0°, 170°W   Zonal Velocity

-100   -60   -20   20   60   100   cm s⁻¹

AUG   SEP   OCT   NOV   DEC   JAN   FEB   MAR   APR
1996   1997